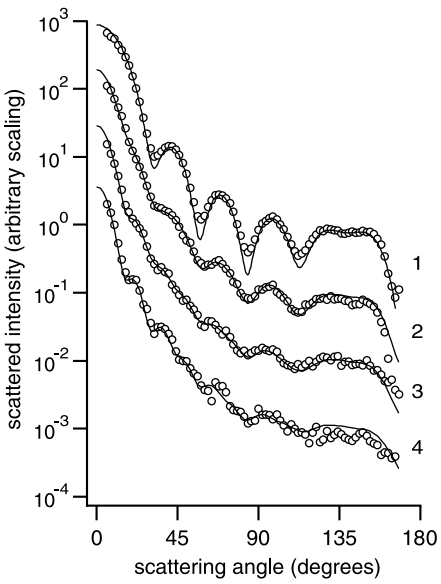

Fig. 4. Intensity of scattered light (488 nm) as a function of scattering angle for dispersions of the first four clusters. Solid lines are calculations of the theoretical scattering from randomly oriented idealized packings of 844-nm spheres (*31*). The data and curves are offset for clarity. Curve 1, single spheres; 2, sphere doublets; 3, triangles; 4, tetrahedra. The agreement between theory and experiment shows that the clusters are well separated and stable.

ade (*11*). The varied and unusual polyhedra of this sequence illustrate how certain symmetries, including fivefold rotational symmetry, can arise solely from compression and packing constraints and need not require interparticle attractions. It may well be possible to define other types of constraints in microsphere systems and in so doing to discover new sphere-packing motifs.

References and Notes

1. J. H. Conway, N. J. A. Sloane, *Sphere Packings, Lattices, and Groups* (Springer, New York, ed. 3, 1999).
2. T. C. Hales, *Discrete Comput. Geom.* **17**, 1 (1997).
3. T. C. Hales, *Discrete Comput. Geom.* **18**, 135 (1997).
4. L. Fejes-Tóth, *Regular Figures* (Macmillan, New York, 1964).
5. H. Reichert *et al.*, *Nature* **408**, 839 (2000).
6. T. Schenk, D. Holland-Moritz, V. Simonet, R. Bellissent, D. M. Herlach, *Phys. Rev. Lett.* **89**, 075507 (2002).
7. K. F. Kelton *et al.*, *Phys. Rev. Lett.* **90**, 195504 (2003).
8. D. R. Nelson, F. Spaepen, *Solid State Phys.* **42**, 1 (1989).
9. A. J. Liu, S. R. Nagel, *Nature* **396**, 21 (1998).
10. C. S. O'Hern, S. A. Langer, A. J. Liu, S. R. Nagel, *Phys. Rev. Lett.* **86**, 111 (2001).
11. N. J. A. Sloane, R. H. Hardin, T. D. S. Duff, J. H. Conway, *Discrete Comput. Geom.* **14**, 237 (1995).
12. Polydispersity is defined as the relative standard deviation in the particle size distribution.
13. Materials and methods are available as supporting material on *Science* Online.
14. B. R. Saunders, B. Vincent, *Adv. Colloid Interface Sci.* **80**, 1 (1999).
15. M. S. Wolfe, C. Scopazzi, *J. Colloid Interface Sci.* **133**, 265 (1989).
16. S. Levine, B. D. Bowen, S. J. Partridge, *Colloids Surf.* **38**, 325 (1989).
17. R. Hinton, M. Dobrota, *Density Gradient Centrifugation*, vol. 6, part 1, of *Laboratory Techniques in Biochemistry and Molecular Biology* (Elsevier/North-Holland, New York, 1976).
18. N. W. Johnson, *Can. J. Math.* **18**, 169 (1966).
19. J. D. Bernal, *Nature* **185**, 68 (1960).
20. R. E. Williams, *Inorg. Chem.* **10**, 210 (1971).
21. M. R. Hoare, P. Pal, *Adv. Phys.* **20**, 161 (1971).
22. F. Spaepen, *Nature* **408**, 781 (2000).
23. R. Hidalgo-Álvarez *et al.*, *Adv. Colloid Interface Sci.* **67**, 1 (1996).
24. U. Betke, M. Henk, J. M. Wills, *Discrete Comput. Geom.* **13**, 297 (1995).
25. J. M. Wills, *Math. Intell.* **20**, 16 (1998).
26. A. Boerdijk, *Philips Res. Rep.* **7**, 303 (1952).
27. B. W. Clare, D. L. Kepert, *Proc. R. Soc. London Ser. A* **A405**, 329 (1986).
28. J. Aizenberg, P. V. Braun, P. Wiltzius, *Phys. Rev. Lett.* **84**, 2997 (2000).
29. Y. D. Yin, Y. N. Xia, *Adv. Mater.* **13**, 267 (2001).
30. M. M. Takayasu, F. Galembeck, *J. Colloid Interface Sci.* **202**, 84 (1998).
31. D. W. Mackowski, M. I. Mishchenko, *J. Opt. Soc. Am. A* **13**, 2266 (1996).

32. We thank V. Breedveld and D. Roux for helpful discussions. Supported by NSF under grant numbers CTS-0221809 and DGE-9987618 and by Unilever Corporation.

Supporting Online Material

www.sciencemag.org/cgi/content/full/301/5632/483/DC1
Materials and Methods
References

28 April 2003; accepted 18 June 2003

Cell Therapy of α-Sarcoglycan Null Dystrophic Mice Through Intra-Arterial Delivery of Mesoangioblasts

Maurilio Sampaolesi,[1] Yvan Torrente,[2] Anna Innocenzi,[1] Rossana Tonlorenzi,[1] Giuseppe D'Antona,[3] M. Antonietta Pellegrino,[3] Rita Barresi,[4] Nereo Bresolin,[2,5] M. Gabriella Cusella De Angelis,[1,3] Kevin P. Campbell,[4] Roberto Bottinelli,[3] Giulio Cossu[1,6,7]*

Preclinical or clinical trials for muscular dystrophies have met with modest success, mainly because of inefficient delivery of viral vectors or donor cells to dystrophic muscles. We report here that intra-arterial delivery of wild-type mesoangioblasts, a class of vessel-associated stem cells, corrects morphologically and functionally the dystrophic phenotype of virtually all downstream muscles in adult immunocompetent α-sarcoglycan (α-SG) null mice, a model organism for limb-girdle muscular dystrophy. When mesoangioblasts isolated from juvenile dystrophic mice and transduced with a lentiviral vector expressing α-SG were injected into the femoral artery of dystrophic mice, they reconstituted skeletal muscle in a manner similar to that seen in wild-type cells. The success of this protocol was mainly due to widespread distribution of donor stem cells through the capillary network, a distinct advantage of this strategy over previous approaches.

There are currently three main experimental approaches to therapy of muscular dystrophies (*1*). Gene therapy focuses on the development of new vectors capable of delivering efficiently the missing gene to the postmitotic nuclei of the muscle fibers in vivo. The pharmacological approach aims to restore the protein complex that is altered in many forms of muscular dystrophy through different strategies ranging from skipping mutated exons to increasing the synthesis of cognate proteins such as utrophin. The cell therapy approach aims to functionally rescue the tissue by delivery of cells (*2*); these may be satellite cells (which regenerate new fibers after damage to the muscle) or pluripotent stem cells (which have been shown to differentiate into skeletal muscle both in vitro and in vivo). However, the limited self-renewal and migratory capacity of dystrophic satellite cells and our modest knowledge of stem cell biology have so far hampered the success of the cell therapy approach.

We recently identified a class of vessel-associated fetal stem cells that can differ-

[1]Stem Cell Research Institute, H. S. Raffaele, Via Olgettina 58, 20132 Milan, Italy. [2]Department of Neurological Science, Istituto di Ricovero e Cura a Carattere Scientifico (IRCCS), Centro Dino Ferrari, Ospedale Maggiore Policlinico, Via F. Sforza 35, 20122 Milan, Italy. [3]Department of Experimental Medicine, University of Pavia, Via Forlanini 6, 27100 Pavia, Italy. [4]Howard Hughes Medical Institute, Department of Physiology, Biophysics and Neurology, University of Iowa College of Medicine, Iowa City, IA 52242, USA. [5]IRCCS E. Medea, Bosisio Parini, 23842 Lecco, Italy. [6]Department of Histology and Medical Embryology, University of Rome "La Sapienza," Via A. Scarpa 14, 00161 Rome, Italy. [7]Institute of Cell Biology and Tissue Engineering, San Raffaele Biomedical Science Park of Rome, Via Castel Romano 100, 00128 Rome, Italy.

*To whom correspondence should be addressed. E-mail: cossu.giulio@hsr.it

entiate into most mesoderm (but not other germ layer) cell types when exposed to certain cytokines or to differentiating cells of a mesodermal tissue. We termed these cells "mesoangioblasts" (*3*). Mesoangioblasts can be grown extensively in culture (more than 50 passages), yet they are growth inhibited at confluence, do not grow in soft agar, and are not tumorigenic in nude mice assays (*4*). Different clonal lines of mesoangioblasts show similar, although nonidentical, growth and differentiation potential: When subjected to microarray analysis, they show profiles of gene expression that not only are similar among themselves, but also resemble those recently reported for hematopoietic, neural, and embryonic stem cells (*5, 6*). In keeping with their differentiation potential, mesoangioblasts predominantly express genes enriched in mesoderm, some of which are receptors and signaling molecules for mesoderm, inducing molecules such as bone morphogenetic protein (BMP), Wnt, and Notch (*7*).

When injected into the blood circulation, mesoangioblasts accumulate in the first capillary filter they encounter and are able to migrate outside the vessel, but only in the presence of inflammation, as in the case of dystrophic muscle. Indeed, mesoangioblasts express many receptors for inflammatory cytokines and are able to migrate in vitro and in vivo in response to HMGB-1 (*8*), a nuclear protein that is released by necrotic cells and acts as a potent inflammatory cytokine (*9*). We thus reasoned that if these cells were injected into an artery, they would accumulate into the capillary filter and from there into the interstitial tissue of downstream muscles.

To test this possibility, we injected 5×10^5 [^{14}C]thymidine-labeled (*10*) wild-type mesoangioblasts into the right femoral artery (*11*) of 1-month-old α-SG null mice ($n = 2$) (*12*). After 24 hours, 30 ± 7% of the injected cells were detected in the muscles downstream of the injected artery, whereas <3% of donor cells were detected in the same muscles when injection had occurred through the tail vein ($n = 2$) or intramuscularly ($n = 2$). Tissue distribution of donor cells was analyzed 24 hours after injection through the femoral artery ($n = 4$); 1,1′-dioctadecyl-3,3,3′,3′-tetramethylindocarbocyanine perchlorate (DiI)–labeled mesoangioblasts were detected outside the vessel wall and within the extracellular matrix of all downstream skeletal muscles, especially in areas where degeneration and regeneration were occurring (fig. S1A). Analysis of serial sections throughout the muscle length (fig. S1C) revealed that DiI-labeled cells accumulated mainly in the quadriceps (3.1 ± 0.4‰ of total nuclei, $n = 2$), gastrocnemius (2.3 ± 0.3‰, $n = 2$), and soleus (1.2 ± 0.2‰, $n = 2$) and to a lesser extent in other muscles such as the tibialis anterior (0.8 ± 0.2‰, $n = 2$) and extensor digitorum longus (EDL) (0.3 ± 0.1‰, $n = 2$). In contrast, satellite cells from transgenic mice ubiquitously expressing green fluorescent protein (GFP) (*13*), delivered through the femoral artery ($n = 4$), could not cross the endothelial layer and remained adherent to the vessel wall (fig. S1B). When male mesoangioblasts, previously labeled with a lentiviral vector expressing nuclear LacZ (*14*), were injected into the femoral artery of female α-SG null mice ($n = 3$), polymerase chain reaction analysis of two reporter genes (*Sry* and *LacZ*) confirmed the presence of the host cells in all the hindlimb skeletal muscles analyzed 2 weeks after injection, but not in the diaphragm (fig. S1D). At this time, foci of mesoangioblasts were mainly located in the microcapillary network, as revealed by fluorescence in situ hybridization (FISH) analysis of the Y chromosome (*15*) of male wild-type mesoangioblasts (fig. S1E, arrows) injected into α-SG null female mice. Several regenerating, centrally nucleated fibers showed the presence of Y chromosome–positive nuclei underneath the fiber basal lamina (double arrows in inset, fig. S1E); both FISH and immunostaining with antibodies to β-galactosidase identified positive nuclei in the center of regenerating fibers (arrowheads, fig. S1, E and F). Several DiI-labeled mesoangioblasts were detected at the periphery of fibers, where they expressed M-cadherin (fig. S1G) and c-Met (*16*), typical markers of satellite cells (*17*). Similarly labeled mesoangioblasts were also detected in several vessels near areas of regeneration, where they expressed α–smooth muscle actin (arrowhead, fig. S1H) or platelet endothelial cell adhesion molecule (arrowheads, fig. S1, I and J); other labeled mesoangioblasts that did not express these markers were also present in the sections (arrows, fig. S1, I and J). These results show that mesoangioblasts can diffuse from the arterial tree into skeletal muscle, where they are incorporated into regenerating fibers or express markers of smooth muscle, satellite cells, or endothelium in vivo.

Restoration of α-sarcoglycan and dystrophin-glycoprotein complex by wild-type mesoangioblasts. We next investigated whether injection of wild-type mesoangioblasts in the muscles of α-SG null mice may restore expression of α-SG and of the whole dystrophin complex (*18*). Two months after a single injection of 5×10^5 wild-type male mesoangioblasts ($n = 4$) into female α-SG null mice, many areas of the quadriceps, tibialis anterior, soleus, gastrocnemius, and EDL expressed α-SG, whereas the protein was completely absent from the muscles of the untreated null mouse (an example for the quadriceps is shown in Fig. 1A). FISH analysis revealed male nuclei adjacent to α-SG–positive membrane (Fig. 1B) and longitudinal sections, which allowed us to estimate that α-SG expression extended for at least 50 μm away from the last Y chromosome–positive nucleus detected, consistent with a certain mobility of the protein within the plasma membrane and outside of the transcriptional domain of a specific nuclear cluster. Transverse sections of control, α-SG null, and treated α-SG null muscle at higher magnification confirmed the reliability of the method used (Fig. 1B).

All the muscle fibers that expressed α-SG after mesoangioblast injection also expressed β-, γ-, and δ-sarcoglycans and dystrophin (an example is shown for the soleus in Fig. 1C). Western blot analysis performed on similarly treated mice ($n = 3$) confirmed the presence of the α-SG protein in skeletal muscle of α-SG null mice treated with wild-type mesoangioblasts. Protein expression in membrane fractions of gastrocnemius or quadriceps from treated mice was comparable to that in wild-type muscles (Fig. 1D). A similar pattern was maintained up to at least 3 months after a single mesoangioblast injection. Comparable levels of integrin β1 subunit and myosin heavy chain (MyHC) were detected in all the different samples analyzed (Fig. 1D). Taken together, these results show that intra-arterial mesoangioblast delivery was effective in restoring expression of α-SG protein and of the other members of the dystrophin-glycoprotein complex in treated α-SG null mice. No immune reaction occurred against reconstituted fibers, even though low-titer serum antibodies to α-SG were detected in treated mice (fig. S2A). On the basis of our previous data, we predicted that very few mesoangioblasts might have reached other muscles (such as those of the noninjected leg or the body wall), and consequently few if any α-SG–positive fibers should be present in these muscles. Immunofluorescence analysis of the corresponding muscles of the contralateral leg and of the diaphragm in the same injected mice revealed rare α-SG–positive fibers (*16*). Several sparse Y chromosome–positive undifferentiated donor cells persisted in the liver and lung 2 months after intrafemoral injection (*16*).

Long-term effect of donor wild-type mesoangioblasts. We then injected 5×10^5 male wild-type mesoangioblasts three times (at 40-day intervals) into the femoral artery of 2-month-old α-SG null female mice ($n = 6$). Animals were analyzed 4 months after the first injection (at 6 months of age). Histological analysis of skeletal muscle tissue

of mice treated by three injections showed an increased number of apparently normal fibers and reduction of the necrotic areas and of cellular infiltrates (Fig. 2A). Consistent with the histology, immunofluorescence analysis revealed the widespread presence of α-SG throughout the whole soleus muscle (more than 50% of the fibers), in contrast with the total absence of signal in untreated α-SG null mice (fig. S3A). We found markedly decreased uptake of Evans Blue dye in skeletal muscle of α-SG null mice treated with mesoangioblasts relative to untreated mice (Fig. 2B), demonstrating a preserved integrity of the sarcolemma (*18*). Finally, staining with Azan Mallory revealed a marked reduction of the fibrosis (stained in blue by the dye) in the muscles of treated mice (Fig. 2C). Even after

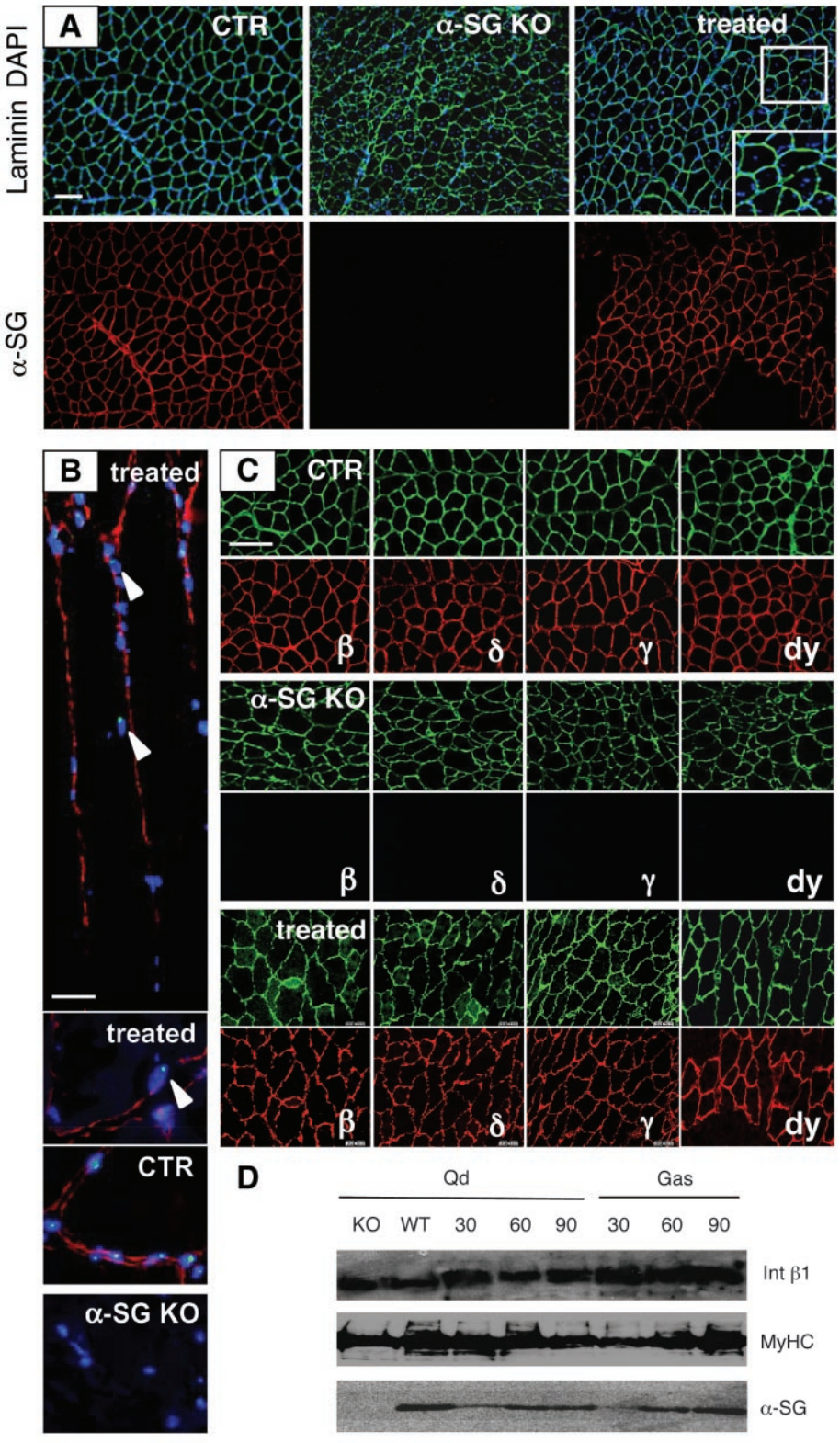

Fig. 1. Expression of α-SG and other dystrophin-associated proteins in α-SG null mice after intra-arterial delivery of wild-type mesoangioblasts. (**A**) Low magnification of quadriceps from control (CTR) mice (left), α-SG null (α-SG KO) mice (center), and treated α-SG null mice (injected with wild-type mesoangioblasts 2 months before killing) (right). Large areas of the treated muscle expressed α-SG after staining with a specific antibody (red). Sections were also stained with antibodies to laminin (green) and with 4′,6′-diamidino-2-phenylindole (DAPI) (blue). Inset: Higher magnification of treated muscle with centrally located nuclei. (**B**) Longitudinal (upper) and transverse (lower) sections of the tibialis anterior of treated mice stained with antibodies to sarcoglycan (red) and hybridized with a probe recognizing the Y chromosome (green). Sections were also stained with DAPI. The merged images reveal donor Y chromosome–positive nuclei (arrowheads) adjacent to α-SG–positive membranes. Sections from wild-type male (CTR) and α-SG null female (α-SG KO) mice are also shown as controls. (**C**) High magnification of soleus from the same treated mice reveals extensive reconstitution of the dystrophin complex after double staining with antibodies to laminin (green, upper panels) or to sarcoglycans and dystrophin (dy) (red, lower panels). (**D**) Western blot analysis of proteins isolated from a postnuclear membrane fraction of two large muscles (quadriceps and gastrocnemius) from α-SG null mice 30, 60, and 90 days after injection of wild-type mesoangioblasts. The filters were reacted with antibodies to α-SG (*12*); MyHC (*3*) and β1 integrin are shown as internal controls. Scale bar, 100 μm (A and C), 20 μm (B).

three consecutive injections, very few α-SG–positive fibers were present in the contralateral soleus (fig. S3C). Consistent with the immunofluorescence analysis, Western blot revealed significant accumulation of α-SG protein at high level in the treated right quadriceps but undetectable levels of the protein in the contralateral untreated left quadriceps (fig. S3B).

Complete functional recovery of treated muscle. The physiology of hindlimb muscles was studied in 6-month-old α-SG null mice treated with three injections of wild-type mesoangioblasts, and the results obtained indicate that the amelioration of skeletal muscle morphology sustains a recovery of function. Previous studies have suggested that functional analysis of whole skeletal muscles in vitro is not a sensitive approach to showing impairment of skeletal muscle function in α-SG null mice. In fact, notwithstanding a clear impairment in animal motility, tetanic force of whole muscles of α-SG null mice was not significantly decreased (*12*).

To better assess skeletal muscle function, we dissected a large population (n = 277) of individual muscle fibers from gastrocnemius muscles of control (n = 3), α-SG null (n = 3), and mesoangioblast-treated α-SG null (n = 3) mice, and measured their cross-sectional area (CSA), specific force (Po/CSA), and maximum shortening velocity (Vo) (Fig. 3, A and B). All fibers used were identified on the basis of MyHC isoform composition (*19, 20*). Because the large majority of fibers contained MyHC-2B (~80%), only type 2B fibers were used for comparison. The analysis of the distribution of CSAs in the three populations of fibers revealed an increase in fiber size in α-SG null mice relative to control mice, as well as a partial recovery of normal size in treated α-SG null mice (Fig. 3B). The median of CSAs was higher for α-SG null mice (5066 μm^2) than for controls (3472 μm^2) and was intermediate for treated α-SG null mice (3922 μm^2); a similar trend was also clear for the 75th percentile (8074 μm^2 for α-SG null mice, 4983 μm^2 for control mice, and 5654 μm^2 for treated α-SG null mice). Finally, both the range of CSAs between the 25th and 75th percentile and the smallest and largest CSA values strongly suggest that the range of variability of CSAs was larger for α-SG null mice than for controls and was intermediate for treated α-SG null mice. Po/CSA was significantly lower ($P < 0.001$) in single muscle fibers from α-SG null mice (42.01 ± 21.63 kN/m^2, n = 106) than in single muscle fibers from controls (61.76 ± 24.80 kN/m^2, n = 82). Po/CSA significantly ($P < 0.001$) recovered to normal values in treated α-SG null mice (65.48 ± 27.02 kN/m^2, n = 89). (For more details of the mean Po/CSA values of the fibers from each animal, see table S2.) No difference was found in Vo among the three fiber groups. Because all fibers were type 2B fibers, the latter result is fully consistent with the well-known dependence of Vo on MyHC isoform composition (*21*). The lack of difference for Vo suggests that neither muscular dystrophy nor mesoangioblast treatment affected the kinetics of actomyosin interaction (*22*). Morphometric analysis of centrally nucleated (i.e., regenerating) fibers indicated that treated mice had a size distribution different from that of untreated dystrophic mice (Fig. 3C). Large, degenerating fibers were absent and a single-mode distribution comparable with normal fibers was observed, which suggests that when regenerating fibers incorporate mesoangioblasts, they are less susceptible to further degeneration.

We also counted the total number of fibers in soleus muscles from control (n = 4), α-SG null (n = 4), and treated α-SG null mice (n = 4). Cross cryosections of soleus muscles from the right leg (the treated leg in the treated α-SG null mice) were stained with hematoxylin and eosin (H&E). Care was taken to cut sections that extended to the edge of muscles. Two sections from the portion of the muscle with the largest CSA were chosen for analysis. A significant decrease (–43.42 ± 4.98%) of total fiber number ($P < 0.0004$) was observed in α-SG null mice (n = 460.05 ± 40.57) relative to control mice (n =

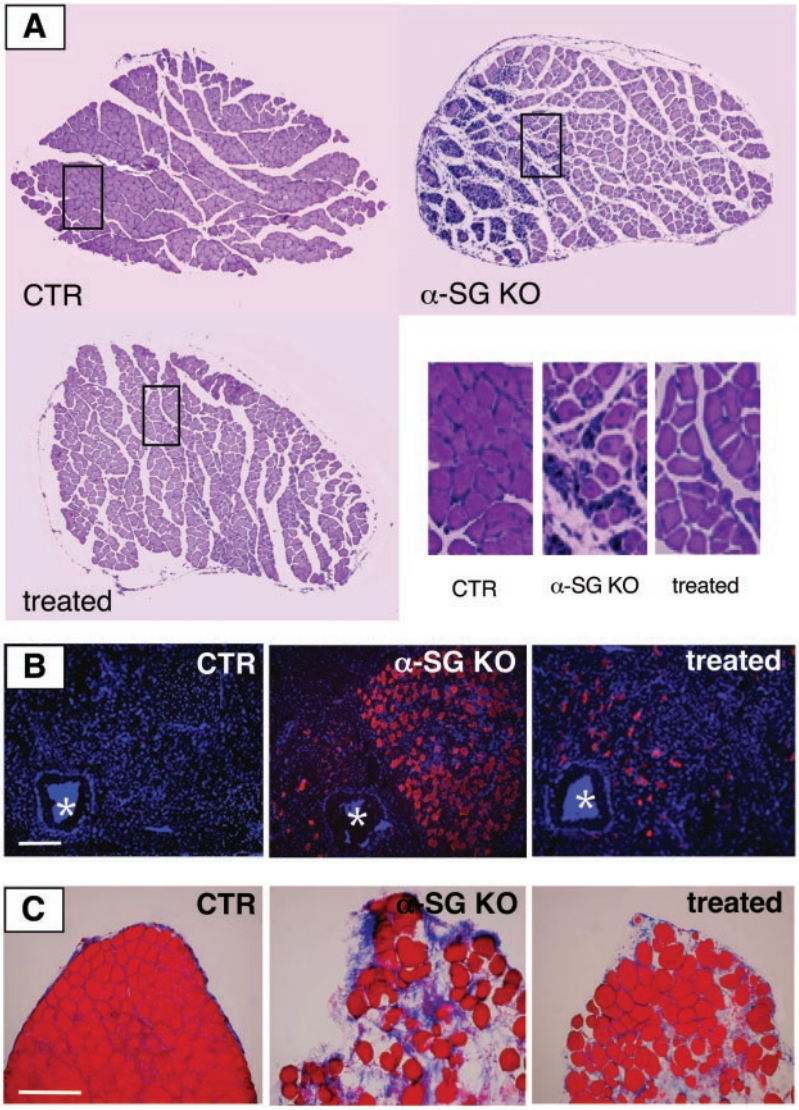

Fig. 2. Morphology of long-term treated α-SG null dystrophic muscles after three consecutive injections of wild-type mesoangioblasts. (**A**) H&E staining of the soleus of a 6-month-old control wild-type (CTR) and similarly aged α-SG null mice (α-SG KO) and treated α-SG null mice. Higher magnification of the sections is also shown. The untreated dystrophic muscle showed a large area of necrosis and disrupted morphology that was significantly reduced after treatment. (**B**) Evans Blue dye injection into the tail vein. Red identifies damaged fibers that have taken up the dye; nuclei are revealed in blue by DAPI staining; tibial bone is marked with a white star. (**C**) Azan-Mallory staining reveals accumulation of extracellular scar tissue (blue). Scale bars, 100 μm.

813.75 ± 92.84). A significant ($P < 0.004$) recovery (+55.97 ± 23.59%) of total fiber number was observed in treated α-SG null mice (n = 718.25 ± 108.64) relative to α-SG null mice, suggesting a more effective regeneration of muscle fibers. At 6 months of age, dystrophic mice show reduced motility in the cage; in contrast, treated mice maintained a certain degree of spontaneous motility despite a monolateral treatment. To quantify the extent of residual motility, we tested control, dystrophic, and mesoangioblast-treated dystrophic mice (n = 4 for each group) by forced run on the rotarod (*23*) at a fixed speed (1.6 m/min for 4 min; 2 min run + 1 min rest + 2 min run). On average, the control mice fell off the rotarod only 3.5 (±1.29) times during the 4-min test and never stopped running before the end of the test. The α-SG null mice could hardly run on the rotarod [i.e., fell off 12.25 (±2.22) times per minute] and stopped running after 1 min. The treated α-SG null mice fell off 9.75 (±1.71) times per minute and could run for 3 min before stopping. These data suggest that functional recovery of treated muscles led to a partial increase in motility, likely because only one leg had been treated.

Morphological and functional recovery by autologous, genetically corrected mesoangioblasts. To test whether autologous, genetically corrected stem cells may represent a possible model for the therapy of muscular dystrophy, we isolated mesoangioblasts from vessels of juvenile dystrophic mice (15 days). Mesoangioblasts are obtained at much lower frequency from adult than from embryonic vessels and grow at a lower rate (division time, 24 versus 12 hours), but they are equivalent to their embryonic counterparts in terms of gene expression and differentiation potency (*4*). We produced a third-generation lentiviral vector (*14*) expressing the mouse α-SG cDNA and GFP cDNA as a reporter gene (hPGK-GFP–α-SG vector). After 48 hours of virus assembly in 293T packaging cells, we collected the supernatant containing the viral particles and used it to infect mesoangioblasts at a multiplicity of infection (MOI) of 200 for 24 hours. Under these conditions, more than 90% of the cell population was efficiently transduced. Furthermore, 293T cells as well as transduced α-SG null mesoangioblasts efficiently produced the recombinant protein (Fig. 4A) at a level comparable to normal skeletal muscle (*24*), a key requirement for preventing α-SG–dependent cytotoxicity. When α-SG null mesoangioblasts were transduced with this vector, more than 90% of the population expressed GFP without changing their growth rate or acquiring features of transformed cells (*16*). Transduced α-SG null mesoangioblasts efficiently differentiated into myotubes coexpressing GFP and MyHC when cocultured with uninfected C2C12 myoblasts (Fig. 4B). Four months after three intra-arterial injections of 5×10^5 transduced α-SG dystrophic mesoangioblasts, many fibers expressed a strong cytosolic diffuse GFP signal and α-SG on the membrane (Fig. 4C). In contrast, very few GFP–α-SG–positive fibers were detected in the contralateral muscles of the noninjected leg (Fig. 4D). Western blot analysis (Fig. 4E) revealed accumulation of the α-SG protein in the membranes of the α-SG null gastrocnemius muscle treated with genetically corrected mesoangioblasts. After long-term treatment with genetically corrected mesoangioblasts, α-SG null mice had restored specific force in individual fibers of their gastrocnemius muscle (Fig. 4F) and also showed an ameliorated motility on the rotarod test (*16*), similar to the effect observed with dystrophic mice treated with wild-type mesoangioblasts. No immune reaction was detected against the GFP protein, although low-titer antibodies were present in the serum (fig. S2B). Indeed, immunostaining with antibodies to MAC-1, which identifies infiltrating macrophages, revealed reduced numbers in the muscles of treated α-SG null mice (fig. S2C).

Future prospects. These data indicate that mesoangioblasts represent a promising approach to cell therapy of primary myopathies. In comparison with skeletal myoblasts, mesoangioblasts show the ability to cross the endothelium and migrate extensively in the tissue interstitium, where they are recruited by regenerating muscle fibers, thus reconstituting the dystrophin-glycoprotein complex. Although this is also the fate of blood-borne progenitors from the bone marrow (*25–29*), the frequency of this event is too low to result in noticeable amelioration of the dystrophic phenotype (*26, 29*). In contrast, mesoangioblasts can be expanded in vitro and directly delivered in large numbers through the arte-

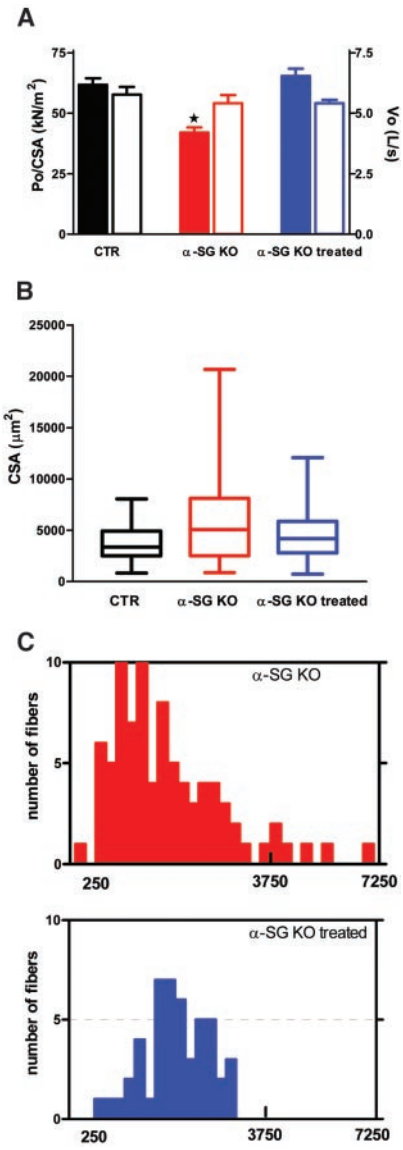

Fig. 3. Functional properties and cross-sectional areas of individual muscle fibers of long-term treated α-SG null dystrophic muscles after three consecutive injections of wild-type mesoangioblasts. (**A**) Specific tension (Po/CSA) and maximum shortening velocity (Vo), and (**B**) distribution of cross-sectional areas (CSAs) of a population of 277 single muscle fibers isolated from gastrocnemius muscles of CTR mice (n = 3), α-SG null mice (n = 3), and treated α-SG null mice (n = 3). Methods for determining CSA, force (Po), and Vo of isolated muscle fibers are described in detail in the online supplement (*19, 20*). As in all mice studied, the large majority of fibers (~80%) from gastrocnemius muscles contained MyHC-2B; only type 2B fibers were used for comparison. In (A), mean values of Po/CSA (solid bars) and Vo (open bars) are shown for type 2B single skinned muscle fibers from the three groups of mice: CTR (black bars), α-SG KO (red bars), and treated α-SG KO (blue bars). Po/CSA values were significantly lower in α-SG KO mice than in CTR and treated α-SG KO mice, as indicated by the asterisk. [Statistical significance of the differences between mean values of Po/CSA and of Vo was assessed by one-way analysis of variance (ANOVA) followed by the Student-Newman-Keuls test to determine which groups were significantly different ($P < 0.05$) from the others.] Details of the Po/CSA values and of animal-to-animal variation are reported in the online supplement. In (B), the box-and-whiskers plot shows the median of CSAs or 50th percentile (indicated by the line in the middle of the box), the 75th percentile (i.e., the top of the box), the range of CSAs (i.e., the width of the box), and the smallest and largest CSAs (i.e., the top and bottom of the whiskers). (**C**) Distribution of CSA values of centrally nucleated (i.e., regenerating) muscle fibers from α-SG KO (upper histogram, red bars) and treated α-SG KO mice (lower histogram, blue bars) determined on H&E-stained cross cryosections of bundles of gastrocnemius muscles from three mice per group.

rial circulation, with no need for a complex procedure such as bone marrow transplantation. Intra-arterial injections are simple and safe procedures in patients where they may be repeated frequently, in contrast to the mouse, where a surgical procedure is required.

In comparison with mesoangioblasts, viral vectors do not cross the endothelium and require intramuscular delivery; they transduce muscle fibers very efficiently, but only in the injected area because of their limited diffusion (*30, 31*). Finally, a number of studies indicate amelioration of the dystrophic phenotype by expression of biologically active molecules such as insulin-like growth factor–I or neutralizing antibodies for myostatin (*32, 33*). These strategies, which do not lead to gene replacement, may be part of a future combination therapy by preserving muscle integrity and thus improving the efficacy of cell therapies.

Before clinical application of these results can be envisioned, several points remain to be resolved. Human mesoangioblasts have been isolated from fetal vessels but not yet from the patient's own vessels (*4*). Our work with juvenile mice indicates that this will ultimately be possible. Recently described adult mesoderm progenitors (*34*) may also represent a useful source, although it has not been shown that they can cross the vessel wall. As far as gene replacement is concerned, lentiviral vectors still pose safety concerns for future clinical application, even though a clinical trial using these vectors has been approved (*35*); however, the use of muscle-specific promoters active only in postmitotic cells and the addition of suicide genes should improve their safety. Moreover, lentiviral vectors are limited in the size of insert they accommodate, so that for Duchenne muscular dystrophy, microdystrophin (*36*) or a small RNA causing exon skipping (*37*) would have to be used (because full-length dystrophin cDNA is too large). Instead of gene replacement, heterologous mesoangioblasts from fetal vessels could be considered under an appropriate regime of immune suppression, if studies in mice should show that only low doses or transient treatment are required.

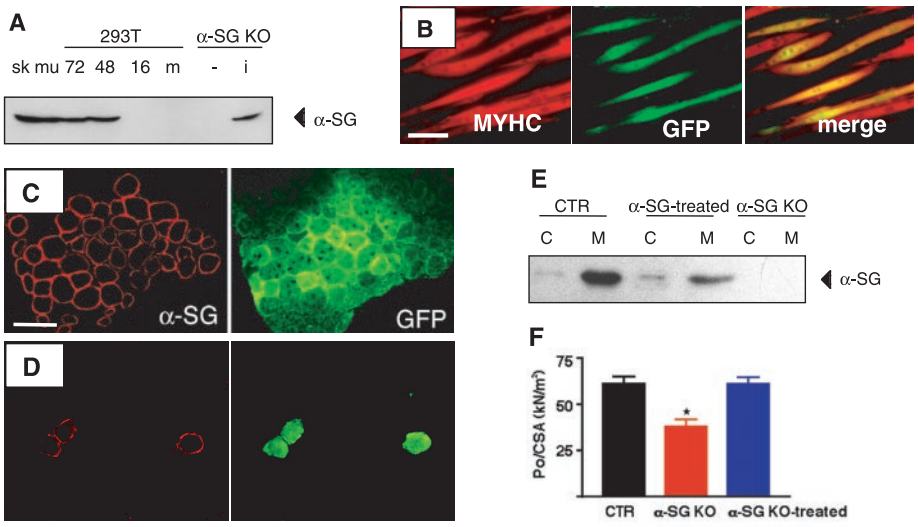

Fig. 4. In vitro gene transfer into dystrophic mesoangioblasts and tissue replacement with transduced cells. (**A**) Western blot analysis of packaging 293T (at 72, 48, and 16 hours after transfection), mock transfected (m), and α-SG null mesoangioblasts either untreated (-) or transduced (i) with a third-generation lentiviral vector expressing α-SG cDNA under the transcriptional control of the PGK promoter and followed by an IRES (internal ribosomal entry site)–GFP, reacted with a monoclonal antibody to α-SG (sk mu, α-SG from skeletal muscle). (**B**) Immunofluorescence analysis of a coculture of transduced mesoangioblasts with control C2C12 myoblasts, showing a large number of MyHC/GFP–positive myotubes that incorporated GFP–positive mesoangioblasts. Scale bar, 10 μm. (**C**) Immunofluorescence with antibodies to α-SG (red) of the gastrocnemius muscle injected three times with 5×10^5 dystrophic, transduced mesoangioblasts through the femoral artery revealed many α-SG/GFP–positive fibers (green). Scale bar, 100 μm. (**D**) Immunofluorescence with antibodies to α-SG (red) of the contralateral, noninjected gastrocnemius muscle revealed very few α-SG/GFP–positive fibers (green). (**E**) Western blot analysis of proteins isolated from postnuclear membrane (M) and cytosolic (C) fractions of the quadriceps muscles from α-SG null mice injected three times with 5×10^5 dystrophic, transduced mesoangioblasts through the femoral artery. The same fractions from control (CTR) and dystrophic (α-SG KO) untreated mice are also shown. (**F**) Specific tension (Po/CSA) of single muscle fibers ($n = 95$) of gastrocnemius muscles from CTR mice (black bar), α-SG null mice (red bar), and α-SG null mice treated with transduced mesoangioblasts (blue bar). Po/CSA values were significantly lower in α-SG KO mice than in CTR and treated α-SG KO mice, as indicated by the asterisk. Details of the Po/CSA values and of animal-to-animal variation are reported in the online supplement.

References and Notes

1. D. Skuk, J. T. Vilquin, J. P. Tremblay, *Curr. Opin. Neurol.* **15**, 563 (2002).
2. G. Cossu, F. Mavilio, *J. Clin. Invest.* **105**, 1669 (2000).
3. M. G. Minasi *et al.*, *Development* **129**, 2773 (2002).
4. M. Sampaolesi *et al.*, unpublished data.
5. M. Ramalho-Santos, S. Yoon, Y. Matsuzaki, R. C. Mulligan, D. A. Melton, *Science* **298**, 597 (2002).
6. N. B. Ivanova *et al.*, *Science* **298**, 601 (2002).
7. E. Tagliafico *et al.*, unpublished data.
8. R. Palumbo *et al.*, in preparation.
9. P. Scaffidi, T. Misteli, M. E. Bianchi, *Nature* **418**, 191 (2002).
10. J. R. Beauchamps *et al.*, *J. Cell Biol.* **144**, 1113 (1999).
11. Y. Torrente *et al.*, *J. Cell Biol.* **152**, 335 (2001).
12. P. Duclos *et al.*, *J. Cell Biol.* **142**, 1461 (1998).
13. T. Takada *et al.*, *Nature Biotechnol.* **5**, 458 (1997).
14. G. Condorelli *et al.*, *Proc. Natl. Acad. Sci. U.S.A.* **98**, 10733 (2001).
15. FISH analysis was performed using the kit from Vysis, following manufacturer instructions.
16. M. Sampaolesi *et al.*, data not shown.
17. P. Seale, A. Asakura, M. A. Rudnicki, *Dev. Cell* **1**, 333 (2001).
18. M. Durbey, K. P. Campbell, *Curr. Opin. Genet. Dev.* **12**, 349 (2002).
19. R. Bottinelli, R. Betto, S. Schiaffino, C. Reggiani, *J. Physiol.* **478**, 341 (1994).
20. M. A. Pellegrino *et al.*, *J. Physiol.* **546**, 677 (2003).
21. R. Bottinelli, C. Reggiani, *Prog. Biophys. Mol. Biol.* **73**, 195 (2000).
22. S. Weiss, R. Rossi, M. A. Pellegrino, R. Bottinelli, M. A. Geeves, *J. Biol. Chem.* **276**, 45902 (2001).
23. O. Pansarasa *et al.*, *Eur. J. Appl. Physiol.* **87**, 550 (2002).
24. D. Dressman *et al.*, *Hum. Gene Ther.* **13**, 1631 (2002).
25. G. Ferrari *et al.*, *Science* **279**, 1528 (1998).
26. E. Gussoni *et al.*, *Nature* **401**, 390 (1999).
27. A. Asakura, P. Seale, A. Girgis-Gabardo, M. A. Rudnicki, *J. Cell Biol.* **159**, 123 (2002).
28. M. A. LaBarge, H. M. Blau, *Cell* **111**, 589 (2002).
29. G. Ferrari, A. Stornaiuolo, F. Mavilio, *Nature* **411**, 1014 (2001).
30. C. Dello Russo *et al.*, *Proc. Natl. Acad. Sci. U.S.A.* **99**, 12979 (2002).
31. K. Yuasa *et al.*, *Gene Ther.* **9**, 1576 (2002).
32. E. R. Barton *et al.*, *J. Cell Biol.* **157**, 137 (2002).
33. S. Bogdanovic *et al.*, *Nature* **420**, 418 (2002).
34. Y. Jiang *et al.*, *Nature* **418**, 41 (2002).
35. R. R. MacGregor, *Hum. Gene Ther.* **12**, 2028 (2001).
36. S. Q. Harper *et al.*, *Nature Med.* **8**, 253 (2002).
37. F. De Angelis *et al.*, *Proc. Natl. Acad. Sci. U.S.A.* **99**, 9456 (2002).

38. We thank C. Bordignon, M. Buckingham, and N. Rosenthal for critical reading of the manuscript and helpful suggestions. G.C. dedicates this paper to the late Franco Tatò, whose scientific insights and subtle sense of humor are still sadly missed. Supported by grants from Telethon/Fondazione Zegna, the European Community, Duchenne Parent Project Italia/Compagnia di San Paolo, Muscular Dystrophy Association (USA), Fondazione Istituto Pasteur–Cenci Bolognetti, Associazione Italiana Ricerca sul Cancro, Agenzia Spaziale Italiana, the Association Francoise contra les Myopathies, and the Italian Ministry of Health. K.P.C. is an investigator of the Howard Hughes Medical Institute.

Supporting Online Material

www.sciencemag.org/cgi/content/full/1082254/DC1
Materials and Methods
Figs. S1 to S3
Tables S1 to S3
References

10 January 2003; accepted 18 June 2003
Published online 10 July 2003;
10.1126/science.1082254
Include this information when citing this paper.